

Transmission Grating Spectrometer for Constellation-X

White paper response to NASA solicitation 210S-GBG-06-001

Kathryn Flanagan, John Davis, Ralf Heilmann, David Huenemoerder, Alan Levine, Herman Marshall, Gregory Prigozhin, George Ricker, Mark Schattenburg, Norbert Schulz, (MIT Kavli Institute for Astrophysics and Space Research) & Andrew Rasmussen (SLAC/Stanford). Contact: kaf@space.mit.edu
11 December 2006

1. Introduction and Overview of the Transmission Grating Spectrometer (TGS)

This white paper proposes a transmission grating spectrometer to provide high spectral resolution at low energies, extending down below 0.2 keV. The transmission grating is *blazed*, concentrating the energy among a single set of orders over a limited readout range. Because of its high efficiency, it will exploit subaperturing of the optic, in conjunction with a very high line density, to give resolving power $E/\Delta E \sim 2000$ (HEW). It has several advantages over reflection grating spectrometers considered for Constellation-X: lower mass, significantly relaxed alignment tolerances, insensitivity to polarization, and the fact that all zeroth order photons go to the calorimeter. (Apart from support structure, the transmission grating is substantially transparent to high energy X-rays and does not represent “loss of area” to the calorimeter in the same way that a reflection grating does.) The transmission grating requires 23 times less diffractor area to fabricate than the counterpart reflection spectrometers, and can be done in-house, reducing cost. The spectrometer readout is based on conventional CCD technology adapted to operate with very high speed and low power. The spectrometer introduced in this white paper builds on successful instruments flown for Chandra and Suzaku. There are novel areas that require development, but leveraging of other programs is already in place.

2. Science

The TGS will recover critical science areas for Constellation-X that cannot be achieved with the basic configuration. We illustrate this through simulations of several science investigations focusing on absorption and emission line spectroscopy.

Absorption Spectroscopy

The observation of X-ray absorbers has become an important part of X-ray studies, which include accreting **black hole** properties, state of matter in accreting and isolated **neutron stars**, abundance and ionization fractions in the **interstellar media** of Galaxies including our own, accretion dynamics and outflows in **active galactic nuclei**, and last but not least mass absorption in the **WHIM**.

Low resolution instruments in the past dealt entirely with either broad-band photoelectric absorption or forests of unresolved resonance absorbers. Examples are the cold absorption of foreground interstellar matter and warm absorbers in active galactic nuclei. The availability of high spectral resolving power with Chandra and XMM-Newton added resolved edge and resonance absorption studies, and provided unprecedented plasma diagnostic power and the ability to study matter at a wide range of temperatures and densities. In the current basic design of Constellation-X, spectral resolving power is provided through a microcalorimeter offering a spectral resolution of 2 eV over the X-ray band, amounting to a resolving power of 300 at 0.6 keV. The X-ray band is particularly sensitive to K-shell absorption from high abundance elements like C, N, O, Ne, Mg, Si, S, Ar, Ca, Fe, and Ni as well as L-shell absorption by Fe. The detection and measurement of X-ray absorption features depends very critically on spectral resolving power. For most science applications using resonance absorption spectroscopy, a resolving power substantially exceeding ~ 300 is required. The microcalorimeter provides high enough resolution only above 1 keV. However, the majority of resonance line absorption occurs below 1 keV, which include K-shell transitions from some of the most abundant elements in the local universe, i.e., from C, N, O and Ne, and L-shell absorption from Ca, Fe, and Ni. Beyond the local universe, increasing redshifts also move important higher energy transitions into the soft X-ray band.

The proposed TGS design will recover absorption spectroscopy science in the soft X-ray band. The following series of simulations of the TGS, and comparisons with high resolution spectrometers currently in orbit and the microcalorimeter capability onboard Constellation-X, demonstrate the types of science that are enabled. These simulations are based on a powerlaw source with index of -2 at observed flux levels of

$\log F_x [\text{ergs/s/cm}^2] \sim -12$. The ordinates of the provided figures are photon counts per plotted bin and thus reflects the available photon statistics. Figure 1a features cold and low-ionization X-ray absorbers based on recent Chandra HETG observations. These are usually found in the cold and warm phases of interstellar media, but are also observed in the vicinity of stellar type black holes and are suspected to reside in accretion disks of AGN. The simulation shows the O-K edge of an X-ray source in M31 at a luminosity of several 10^{38} erg/s. It shows the edge at 22.89 Angstrom (0.540 eV) and its O I 1s - 2p(3p) resonances at 23.5(23.1) Angstroms plus similar resonances from O II and O III. While the HETG (blue line) requires about 400 ks exposure to resolve some of the basic features and provide enough contrast for the line equivalent widths, the proposed TGS reveals the entire structure at full contrast with a 40 ks exposure (black line). The microcalorimeter (red line), though superior in effective area, can partially resolve the edge and its O I 1s - 2p feature but is entirely insensitive to any substructure. A similar case can be made for the Ne K and Fe L absorption on the shorter wavelength side as well as for N and C K at the long wavelength side.

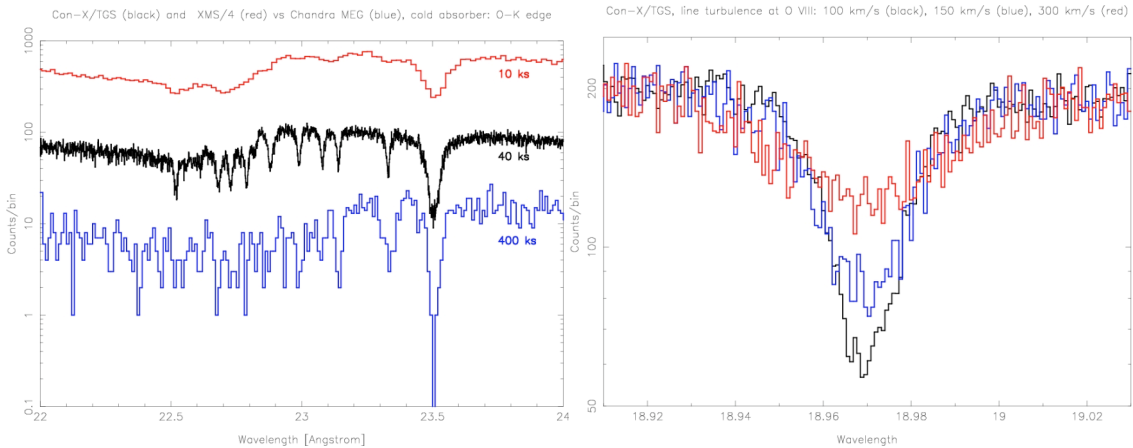


Figure 1a (left) Simulation of O-K edge of an X-ray source in M31. The TGS captures the spectral details in 1/10 the observation time required for the Chandra HETG. The XMS cannot resolve these details. Figure 1b (right) The TGS distinguishes among three velocities differing by 50 km/s in the OVIII resonance absorption line.

Figure 1b demonstrates the ability of the TGS to extend the dynamic range of the absorption depths. The ability to reliably determine dynamic velocities in resonance absorption is a critical element in the diagnostics of absorption in ISMs and the IGM/WHIM, where velocity ranges between 10 and 200 km/s are expected. The simulation shows the O VIII resonance absorption line observed with the proposed TGS at three velocities. The TGS will resolve velocities between 50 and 300 km/s with a sensitivity of 20 km/s.

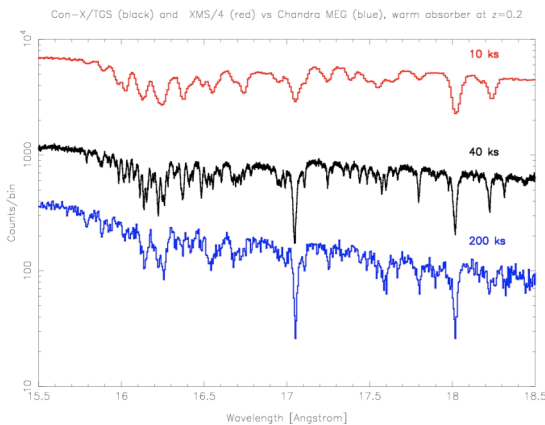


Figure 2 Modest TGS exposures fully resolve warm absorbers from moderately active AGN.

The value of TGS resolution in studying warm absorbers is demonstrated in Figure 2. The simulation shows a warm absorber calculated with XSTAR version 2.1kn6 using an ionization parameter and a column density expected for a moderately active AGN at $z = 0.2$. The wavelength range covers Fe L shell transitions. AGN usually provide substantial ionized columns, but the microcalorimeter, regardless of exposure (red line), can at best partially resolve only some of the absorption, becoming insensitive to the absorber at longer wavelengths. The TGS (black line) exposes the absorber entirely with only moderate exposures. At longer wavelengths, the TGS performance improves, allowing the entire absorber to be observed. Thus, the TGS is sensitive to absorbers at significantly higher redshifts than the basic Con-X can study. The Chandra HETG (blue line) requires

extreme exposures for this type of absorber to resolve the most prominent lines and its efficiency declines dramatically below 20 Å.

In the WHIM, absorbing columns are at least an order of magnitude lower than shown in the simulation of Figure 2. Thus, the microcalorimeter will not be able to detect WHIM absorption from Fe L, O, N, and C. In contrast, with increased exposure, the TGS will be sensitive to columns as much as two orders of magnitude lower than in these simulations for high oscillator strength transitions such as Fe XVII at 15 Å, O VIII at 19 Å, and O VII at 21.6 Å.

Resolving WHIM components is needed in order to determine the ionization balance by comparing to high resolution UV spectra. The lines are expected to be intrinsically narrow, with b values of 50-100 km/s (Fang *et al.*, ApJ 564, 604 (2002)). With high signal observations, such line broadening can be measured using the proposed grating spectrometer design. These spectrally narrow WHIM components can be found within 300-400 km/s of each other (Tripp *et al.*, ApJ 534, L1 (2000)), requiring spectral resolution greater than 1000 to separate components. This grating spectrometer design has the needed resolution.

Emission Line Spectroscopy

High resolution emission line spectroscopy is important to the "Life Cycles of Matter", and particularly "High-Energy Stellar, Protostellar and Protoplanetary Physics". High resolution observations at wavelengths longer than ~ 8 Å (the approximate handoff point between the XMS and the TGS) reveal many astrophysically important features, such as density sensitive He-like triplets which are formed at temperatures and densities relevant to **stars' coronae, disks, winds, and accretion**. In addition, there is a forest of Fe lines from many ion states (XVII-XXIV) which are crucial to resolve for determining temperature structures. Little of these studies of temperature structure and dynamics in stellar structures can be done at XMS resolution, regardless of the high effective area. The XMS will provide valuable constraints, but TGS resolution is fundamental to many important studies. XMS will provide complementary information on diagnostics sensitive to hotter, higher density plasma from lines of Mg, Si, S, Ar, Ca, and from Fe K. TGS will cover Fe XVII-XXIV, Ne, O, N, C. Together they will provide relatively complete characterization of the X-ray spectrum; neither by itself will provide a sufficient characterization. We demonstrate the importance of the TGS with science simulations based on the modeled TGS effective area and spectral resolution. Specific examples are given in the figures below.

High resolution is necessary for accurate measurement of line fluxes by resolving blends and determining the continuum accurately. As shown in Figures 3 and 4, many regions of coronal spectra are very rich in lines and require HEG-like resolution. Even at such resolution, unblended lines are required to scale unresolved blends of the same ion which overlap other lines of interest (such as weak but significant Fe XIX in the Ne IX 13.55 Å intercombination line). The TGS will also provide detailed velocity information, as shown in Figure 5. The TGS can detect velocity shifts of 10 km/s with high significance (3σ , for a known instrumental profile, for a group of lines of known positions), whereas the XMS sensitivity to velocity is 3 times less. The TGS will allow resolution of active **binary star orbital and rotational motion** of stellar coronae, time resolution of flows in stellar flares, and provide sensitive probes of accretion and **disk flows** in young or other **accreting binary systems**. While the XMS can isolate He-like triplets for some lines (O7), or some stars with low iron, some spectral regions have blends which cannot be resolved with XMS. Furthermore, the dynamical effects are below the velocity resolution of XMS, even for the well resolved features.

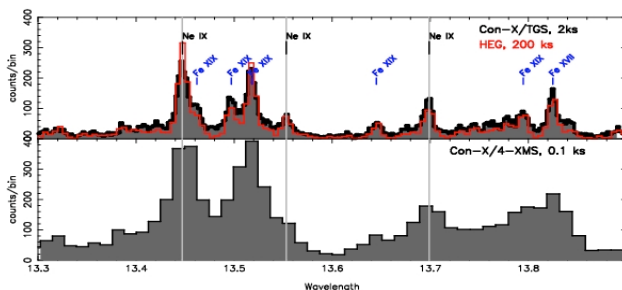


Figure 3 This simulation of Capella, a bright coronally active binary, shows the important Ne IX region of density-sensitive He-like lines. The impact of effective area and spectral resolution is clear – a 2ks observation with the TGS is comparable to a 200ks observation with the Chandra HEG (top). An observation with the XMS (bottom) does not capture details of the spectrum.

is, however, sufficient mass allowance to permit two integrating structures on two different SXTs if the proposed arrangement is difficult to implement.) A drawing of the two arrays on one SXT, and the focal plane layout showing the two CCD readouts is given in Figures 6b and 6c.

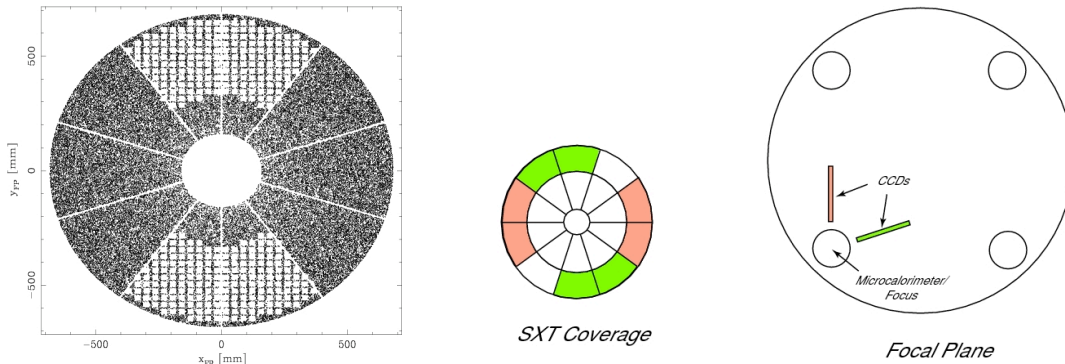


Figure 6 (a) Shadowgram illustrating one TGS array on an SXT. (b) Arrangement of two grating arrays on one SXT. (c) Each grating array has its own readout.

Since the gratings have very high line density (10,000 lines per mm), the high spectral resolution would ordinarily come at a cost of long readout length. However, the gratings are blazed, having very high efficiency (in orders 1 through 5) over a limited range of dispersion angle (see Figure 8). This means that the CCDs need capture only a limited region of the dispersed spectrum. The point of closest approach to the calorimeter is 231 mm, which is clear of the XMS envelope. Each readout requires 20 CCD devices.

The CCDs and gratings are arranged along a Rowland torus, and occupy a 3D envelope as specified in the box below. (The exact envelope depends on the final arrangement.) The placement of the readout electronics assemblies is not critical, provided they are located within ~1 m of the devices. They may even be placed *under* the readout for compact arrangement. The range of diffraction angles is small and will not unduly constrain a postcollimator.

<u>Cost, Mass and Power</u>
Grating Mass: 22.6 kg
CCD Readout Mass: 2x19 kg
Total Mass: 60.6 kg
Total Power: 30W
Gratings cost (FY06): \$39M
Readout Cost (FY06): \$50M

<u>Accommodations</u>
Total grating coverage: 288 degrees on one SXT from $r = 324$ to 659 mm (shells 32-128)
Grating envelope: < 80 mm
Rowland diameter: 9250 mm
Readout range: 25A to 77A; 231 mm to 719 mm from XMS
Readout envelope: < 65 mm
Readout length: 488 mm or 20 CCD devices (each readout)
Dispersion range: 1.46 to 4.42 degrees
Size of electronics boxes: 60cmx15cmx15cm (detector)
30cm x 30cm x20 cm (detector electronics assembly)
30cmx30cmx30cm (DPA, PSMC)
Placement of electronics boxes: PSMC and DPA within 2m,
And DEA within ~1m of detector assembly

In the boxes above, some items should be identified as having been omitted and assumed covered elsewhere. We have not included the mass associated with radiators and solar panels. The grating integrating structure is included, but not attachment hardware for gratings or CCDs. A fid light or position feedback system has not been included. Operations costs have not been included.

a. Technical description of gratings

At the core of the TGS lies a new type of high-efficiency, blazed transmission grating, designated the Critical-Angle Transmission (CAT) grating. Unlike previous transmission gratings (such as the Chandra HETG) it is not a traditional phase grating, but instead achieves high diffraction efficiency over a broad band pass through reflection off of the sidewalls of high aspect ratio (AR) grating bars that are inclined by angle θ less than the critical angle of total external reflection θ_c relative to the direction of the incident x rays. Highly efficient sub-critical-angle reflection and grating diffraction conditions are fulfilled for a wide range of λ satisfying $\theta < \theta_c(\lambda)$. Off-normal incidence at these small angles leads to efficient blazing,

and only orders on one side of the transmitted 0th order beam need to be detected. Higher-energy x rays (where $\theta_c(\lambda) < \theta$) are mostly transmitted (apart from weak absorption by the grating bars) in 0th order and contribute to the calorimeter signal.

Due to the small critical angles for $\lambda \approx 10 - 50$ Å, high AR (~150) grating bars are required. Such high AR structures can be fabricated through the highly anisotropic KOH etching of crystalline silicon, resulting in atomically smooth sidewalls defined by Si (111) lattice planes [Hölke & Henderson, *J. Micromech. Microeng.* **9**, 51 (1999)]. To achieve high angular dispersion we propose a grating period of 1000 Å.

Efficiency modeling of such gratings was done using the GSOLVER software (see Figure 8), which is based on a hybrid rigorous coupled wave and modal analysis [<http://www.gsolver.com/>]. Similar approaches have been used previously to model related existing zone plate structures [Hambach, *et al.*, *Opt. Lett.* **26**, 1200 (2001)]. We find that silicon alone, without a metal coating, will provide high efficiency. Thus, losses of high order efficiency due to deposition of the rougher metal overlayer are eliminated. Our simulations also predict that CAT gratings are highly insensitive to polarization (< 0.25% relative difference in efficiency between TE and TM modes).

The gratings will have a hierarchy of support structures. We assume a 3055 nm thick grating, with an integrated coarse support. (This support structure is thin enough to allow some photons through to zeroth order.) The structure is overlaid with a thick honeycomb. The next level is a 2-dimensional metal frame. The grating facet size will be determined based on raytrace studies and fabrication constraints; the target size is 100 mm with the period varied across the grating to optimize resolving power. Larger structures will be matched to the optic modules through the grating integrating structure to eliminate further throughput losses. Grating parameters and support structure details are listed in the box below.

Grating Parameters
 Period: 1000 Å (10,000 lpmm)
 Thickness: 3055 nm
 Graze angle: 1.5 degrees
 bar-to-period ratio: 0.2
 material: Si
 facet size: 15mm to 100 mm

Support Hierarchy
 Coarse support (1D): integrated 3055 nm thick with 0.1 µm micron line on 2 micron pitch
 Thick honeycomb: 1 mm thick with 50 µm line on 1 mm pitch
 Metal frame (2D): 2 mm thick with 2 mm line on 4 cm pitch

A prototype TGS grating is being developed under a combination of a ROSES grant, student fellowship support, and internal MKI development funds. We are on target to produce a small x-ray tested silicon grating prototype with 1000 Å period, a duty cycle (bar-to-period ratio) of 0.2, and thickness of 3 microns within one year. In the subsequent two years, we will produce full-size gratings and develop the coarse support structure.

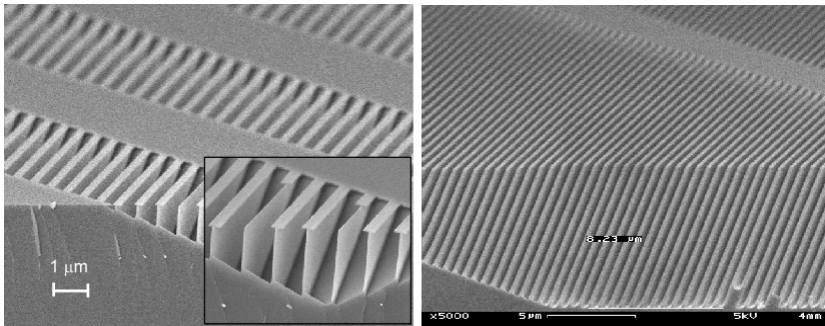
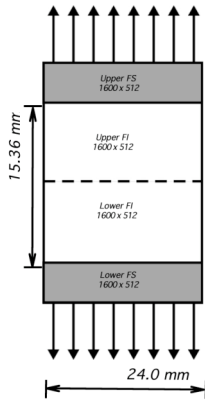


Figure 7 Prototype under development at the Space Nanotechnology Laboratory at MIT. The roughness of the (111) sidewalls was measured by AFM to be 0.2 nm, which should have negligible impact on reflectivity of the side walls.

b. CCD readout description and assumed parameters

The proposed focal plane readout will be comprised of back-illuminated X-ray CCDs fabricated at MIT Lincoln Laboratory (MIT/LL). The CCDs will be based on enhanced, multi-output structures that are similar to those that we have utilized in previous flight programs. The back side treatment will utilize the molecular beam epitaxy (MBE) process recently developed at MIT/LL. The low energy X-ray performance of MBE BI CCDs that we have measured is superior to that of any other known BI CCD technology, both

in terms of energy resolution as well as quantum efficiency. Each CCD in the array will have dual parallel sections, each 1600 columns by 512 rows. The dimensions of the resulting imaging array will be 24.0 mm [dispersion direction] x 15.36 mm [cross dispersion direction]. The image array pixels will be 15 microns x 15 microns, while the frame store pixels will be 7.7 microns by 15 microns. In order to allow high readout speed and low dark current (thus enabling near room temperature operation), each CCD will be partitioned



into 16 blocks, each with its own output, as shown in the figure at left. To increase readout speed even further we can utilize on-chip pixel summation, which will also provide optimum sampling of the TGS PSF. We estimate that a 2 column x 8 row summed "superpixel" with dimensions of 30 microns x 120 microns will be optimal. Summed in this way, the CCD frame rate will be 72 Hz (13.8 ms frame time). The effective "superpixel" size (and the frame rate) can be modified as needed in software to optimize a given observation. We estimate that 20 CCDs will be needed to provide a readout length of 488 mm; the gaps between the CCDs will be 0.4 mm, the same as we achieved for ACIS-S on Chandra. The analog signal processing circuits and digital converters will be edge-mounted as hybrid circuits adjacent to the CCD, allowing for a very fast and low power readout. We estimate that the entire 20 chip long readout will require 15 W of power; 2 such readouts will need 30 W. An optical blocking filter consisting of 100Å of Al will be deposited directly on the surface of the CCDs.

A compact low power hybrid circuit for fast CCD readout funded by internal Lincoln Lab development money is currently being designed, and first samples should be available before the end of this year. The circuitry will be further improved as part of a DARPA funded project intended to develop a space based X-ray shadow mask camera.

4. Performance

a. Effective Area and Bandpass

Efficiency modeling indicates high blazed grating efficiency for ideal incidence angle. In order to obtain a more realistic representation, we considered a grating facet of ~10cm size. The modeled efficiencies are given in Figure 8. With the range of incidence angles expected for such a grating, the peak efficiency was reduced by the "non-optimum" incident angles, but the integrated efficiency was essentially constant – it had virtually no effect on effective area for the instrument. All effective areas used the efficiencies of Figure 8 to be conservative (in lieu of the ideal incidence angle).

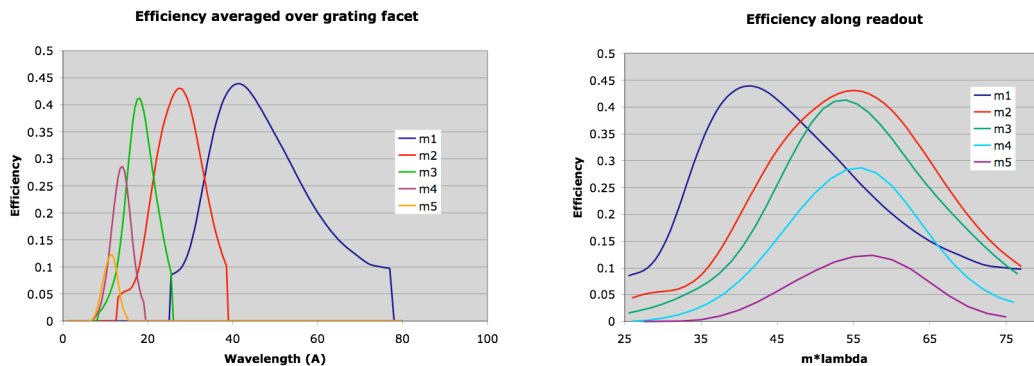


Figure 8 (left) Grating efficiency for orders 1-5 falling on the readout. Efficiencies were modeled with GSOLVER, and include the range of incidence angles expected for a grating facet of ~10 cm. (right) Plot of grating efficiency as a function of $m \cdot \lambda$ (which corresponds to position along the readout) shows that most of the efficiency is captured by CCDs spanning the range $25.5\text{Å} < m\lambda < 77\text{Å}$.

In order to calculate effective area, we considered structural blockage, CCD efficiency and optical blocking filter transmission. We assumed the mirror input model for the 4SXT configuration. (The 3SXT configuration does not meet the Con-X effective area requirement at 6 keV, and we found that the introduction of gratings would exacerbate the problem. Therefore, we did not study that configuration in detail.)

We found that our proposed TGS instrument increases the Con-X bandpass down to ~ 165 eV. It allows the 6 keV system effective area requirement to be met with margin, and the 1.25 keV requirement to be met as well (but without margin). The spectrometer provides 1000 cm^2 of effective area (satisfying $E/\Delta E > 300$) at energies above ~ 320 eV. It is worth noting that even if all four mirrors were completely covered with TGS gratings, the 6 keV effective area requirement would still be met.

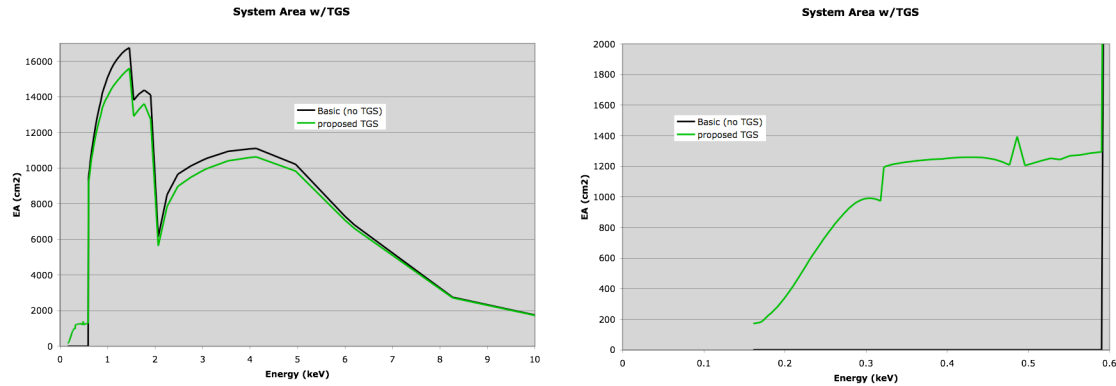


Figure 9 (left) Grating spectrometer reduces system area slightly at energies above 0.6 keV, but meets requirement at 6 keV with margin and at 1.25 keV without margin. (right) The grating spectrometer provides 1000 cm^2 of system area at energies above ~ 320 eV (wavelengths longer than 38.5Å). The instrument energy range goes down to ~ 165 eV, with lower effective area. A longer readout would increase the area at lower energies. Note that only area satisfying $E/dE > 300$ is counted.

b. Spectral Resolving Power

As a starting point, we adapted the Chandra HETG error budget equations to the TGS following Canizares *et al.* PASP, Vol. 117, No. 836, 1114 (2005). We identified the terms expected to significantly impact the spectral resolving power (optic PSF, grating size, observatory level effects) and obtained a preliminary estimate of resolution. Under current fabrication practice, period variations are not expected to significantly impact the spectral resolution. Readout time and CCD pixel size are also insignificant contributors. It is worth noting that alignment and mounting tolerances are *much* looser than for reflection grating schemes, so that gravity sag, thermal distortions etc. are lesser considerations.

The most significant factor in correctly assessing the spectral resolution is the optic. This is even less straightforward under subaperturing. We carried out *two* separate raytraces of the TGS instrument. We

<p><u>Assumed Optic Errors (arcsecs HPD)</u> SXT on-orbit performance: 12.48'' Telescope level effects: 4.1'' comprised of Attitude/knowledge drift: 2'' SXT/SI focal plane drift (thermal): 2'' Telescope mounting strain: 2'' SXT/SI vibration effects: 2'' SXT/SI misalignment (off-axis error): 1'' SXT/SI focus error: 0.2''</p>	<p>we assumed a 12.5 arcsec HPD mirror with slope errors to model the optics, and 4.1 arcsec (2-dimensional HPD) alignment errors to model the Gaussian telescope-level effects. (The breakdown of assumed contributors is given in the box.) In one raytrace, we assumed 15 mm grating facets with uniform period, arrayed with a symmetry axis through the zeroth order. (In practice, we expect to use much larger facets and chirp or vary the period to compensate. Arraying with a symmetry axis through the blaze may improve the resolving power.) This raytrace considered cases where out-of-plane scatter was set to zero or to one-tenth of in-plane scatter. In a second raytrace, a Wolter II optic was modeled without mirror scatter. The gratings were 100 mm facets arranged on an off-center Rowland circle to optimize the spot size at blaze. Based on these two raytraces, we have provisionally accepted a resolving power approximated by $R(\text{HEW}) \sim 44m\lambda(A)$. (The two raytraces bracketed this result.) Figure 10 shows the result. The resolving power is "provisional" because we do not have a mirror model that we can be confident accurately represents the flight optics. Critical to the resolving power estimate is the assumption that slope errors, not alignment errors, dominate the optic PSF. If this is not true, it will negatively impact any grating arrangement employing subaperturing. In addition, the telescope-level effects must be controlled. The limits we have assumed in the box are not unduly restricting. The error budget terms associated with the Constellation-X five arcsecond "goal" PSF will provide a much improved TGS performance. For those who would like to examine how effective this</p>
---	---

proposed instrument would be in achieving specific science goals, response matrices based on our effective area and spectral resolution estimates will be posted at <http://www.space.mit.edu/~kaf/CAT/> in the next few weeks.

A significant contributor to high spectral resolution is the fact that the instrument brings in shorter wavelength at higher orders, increasing the resolving power there. The order-by-order resolving power is shown in Figure 10. Since a given wavelength is captured in multiple orders, an efficiency-weighted resolving power is a useful figure of merit. This is also shown in Figure 10. *Note that the calculated HEW resolving power exceeds 2000.* The mission minimum resolution is no longer defined by a simple cross-over in the two resolution curves, for the grating resolution exceeds the calorimeter resolution at all energies where it has significant effective area. This means that *inclusion of the TGS on Constellation-X will raise the mission spectral resolution*, the minimum being defined by calorimeter performance and system area.

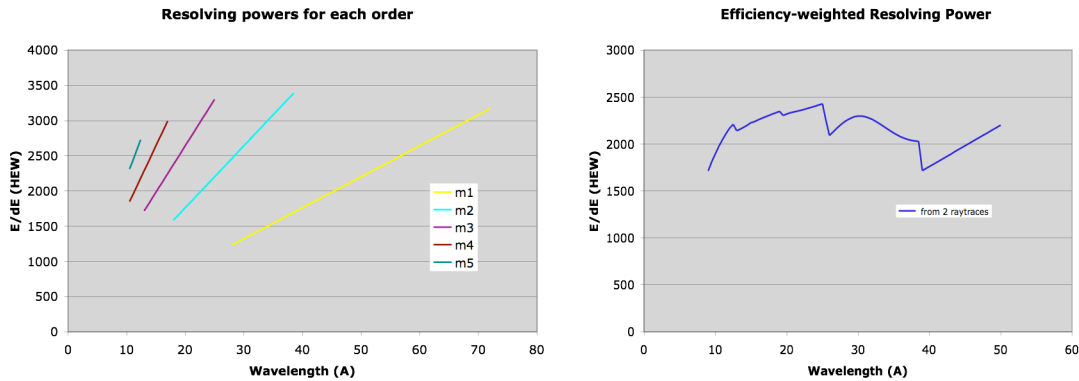


Figure 10 (left) Resolving power (HEW) for each order where efficiency is greater than ~10%. A given wavelength can be captured on the readout in several orders (each order with a different resolving power), so an efficiency-weighted resolving power is shown at right. The values come from two different raytraces and have an error of ~25%. Note that the HEW resolving power is over 2000 (>1300 FWHM resolving power).

The fact that the zeroth order photons are detected by the XMS (with larger pixel size than the CCD) deserves mention. The zeroth order will not impact the spectral resolution itself, but can impact the absolute wavelength scale. The Con-X requirement from the Top Level Requirements Document is “the energy (wavelength) accuracy shall be <20% (TBR) of the energy (wavelength) resolution, with a goal of <10% (TBR).” For our baseline configuration using a Lorentzian form for the grating LSF, we estimate that a line sampled with 4 bins per FWHM and 10 counts peak can be centroided to 0.1*FWHM (and less in proportion to 1/sqrt(max counts)). To obtain the required absolute accuracy of 0.2 times the FWHM, we require the zero order centroid to be comparably good, corresponding to about 0.1 PSF. The XMS sampling is adequate (~3 pixels per resolution element) for counting statistics to dominate the centroid error, and any grating observation will easily have sufficient counts to centroid to at least 0.1 times the PSF. However, to maintain an absolute wavelength scale in order to conduct accurate velocity measurements, there needs to be a reference between the XMS and TGS structures at better than about 0.1*grating FWHM. We have not explicitly made provision in this white paper for instrumentation to provide such a reference, but we are aware of at least one implementation at reasonable cost.

TGS Impact on Mission Performance

- Grating resolution $R(\text{HEW}) > 2000$
- 1000 cm^2 EA above 320 eV
- Mission spectral resolution increased (to ~600, set by XMS)
- 6 keV EA requirement met
- 1.25 keV EA requirement met
- bandpass increased (down to 165 eV)

5. Technology Readiness

a. Experience and Infrastructure of TGS Team

The Space Nanotechnology Laboratory (<http://snl.mit.edu>) has provided transmission gratings for 10 NASA missions (e.g., Chandra, SOHO, IMAGE, GOES, TWINS). It has fabricated 100 nm-period free-standing transmission gratings in the past. Its cleanrooms house the Nanoruler, a unique scanning beam interference lithography system for the rapid high-precision patterning of large substrates, and a number of other lithography and microfabrication tools. As part of the Con-X grating technology development the SNL has achieved record results in the precision patterning of large-area reflection gratings, in blazed reflection grating efficiency (both in-plane and off-plane), and in the flatness of thin large-area reflection grating substrates. SNL staff also has full access to the extensive set of microfabrication and characterization tools of the MIT Nanostructures Lab (NSL) and the MIT Microsystems Technology Laboratories' (MTL) user facilities.

The MIT focal plane readout will be developed at the MIT Kavli Institute by the most experienced team in the world in the area of space-based astronomical X-ray CCD cameras. This skilled team has fabricated the X-ray cameras for: 1) the ACIS instrument on the Chandra X-ray Observatory (launched in 1999); 2) the focal plane instruments on two Japanese satellites, ASCA (launched in 1993) and SUZAKU (launched in 2005); and 3) the SXC instrument on the HETE-2 satellite (launched in 2000). In every instance, these MIT instruments have provided the international astronomical community with excellent data, meeting or exceeding their original performance specifications over the mission's lifetime. For the TGS instrument, the CCD development will be done in a close, well established collaboration with the MIT Lincoln Laboratory (MIT/LL)--again, a facility with the most extensive experience in the world in fabricating high quality X-ray CCDs. The MIT Kavli Institute has the required infrastructure for building, testing and calibrating the proposed focal plane. This infrastructure was developed over many years of developing the previously-mentioned instruments, and includes vacuum chambers, X-ray monochromators and spectrometers, calibrated detectors, pumping stations and X-ray sources. Thus, the MIT Kavli Institute + MIT/LL team is fully prepared to undertake the development of the proposed instrument.

The X-Ray Grating Evaluation Facility (XGEF) was developed to test and calibrate the Chandra HETG transmission gratings, and could be adapted for use with the TGS. This facility provides the capability for acoustic testing, thermal cycling, X-ray efficiency testing, and measurement of period variation and roll.

b. Current TRL level

Gratings:

- Mounting transmission gratings: TRL9
- Free-standing transmission gratings: TRL 9
- 1000 A period (10,000 lines per mm): TRL 4
- Si integrated support structure: TRL 3
- High aspect ratios: TRL 3
- Large-area gratings/Nanoruler: TRL 3
- Chirp/VP-SBIL: TRL 2 (under construction)
- CAT grating concept: TRL 2

CCDs:

- CCDs for the focal plane will be manufactured with conventional technology used at MIT Lincoln Laboratory (MIT/LL) for many spaceflight-proven devices (TRL 10).
- Backside treatment will be based on the MBE process developed at MIT/LL and shown to produce excellent results for X-ray CCDs (TRL 5).

c. Major steps needed to achieve TRL 6

Gratings:

- Implement the already designed and mostly built VP-SBIL upgrade to the Nanoruler
- Implement period-halving scheme
- Fabricate integrated CAT grating cross-support structure
- Achieve mechanically stable high aspect ratio grating bars
- Integrate large-area (> 1"x1") CAT gratings with higher-level support structures
- X-ray tests of large-area CAT gratings

CCDs:

- Reduction of BI dark current to permit near room temperature operation.
- Deposition of very thin light shield directly on the surface of a BI device.
- Improvement of CCD radiation tolerance in the Con-X orbit.
- Implementation of high speed, low power, compact readout circuits which we have been developing in prototype form for a DARPA program.
(All currently at TRL4)